

Self-Organizing Map for surface characterization in time series

Bassam ABDEL LATIF, Grégoire MERCIER and Basel SOLAIMAN
 GET / ENST Bretagne / dpt ITI
 CNRS UMR 2872 TAMCIC / TIME
 Technopôle Brest-Iroise, CS 83818
 F-29238 Brest Cedex 3, France
 Email: Bassam.alatif@enst-bretagne.fr

Rémi LECERF
 COSTEL, IFR CAREN
 CNRS UMR 6554 LETG,
 Université Rennes 2
 Place du recteur H. Le Moal,
 CS 24307, 35043 Rennes cedex, France

Abstract—Monitoring changes in the vegetation cover during the intercrop season is of a special interest in intensive agricultural regions. The presence of bare soils leads to detrimental environmental effects such as soil erosion or water quality degradation. To identify and monitor winter land cover at a regional scale in the Brittany region in France, data from the Moderate Resolution Imaging Spectroradiometer (MODIS) low resolution time series were used. This study examines the Self-Organizing Map (SOM) for classifying winter land cover with MODIS time series in agricultural and fragmented landscapes. Field data and high resolution images have been used to generate two sets of pixels for training and validation. A comparison between the suggested method and NDVI thresholding is presented.

I. INTRODUCTION

The absence of vegetation cover on the agricultural soils during the intercrop season is detrimental for the environment, especially with soils degradation [1] and the deterioration of water quality through the transfer of pollutant fluxes towards rivers [2]. From an environmental point of view, it is necessary to reduce areas with bare soils in intensive farming regions. Planting of intercrops very soon after harvesting is helpful since the vegetation cover can be efficient enough on intense rain events [3]. Considering that the spatial distribution of these areas is not known, the first task to undertake is to identify them precisely, and analyze their interannual spatial variation. First investigations were done using a threshold on MODIS NDVI to discriminate bare soils from covered soils. A relation was found between vegetation cover and MODIS NDVI [4] and permits to identify bare soils from covered soils.

But classifying winter land cover into only two classes is not sufficient for undergoing studies particularly concerning evaluation of soil erosion and organic fertilizer run-off. Moreover, the use of single date image may lead to classification errors because intra-seasonal changes are not taken into account.

The spectral behavior of various winter agricultural land cover is very similar. As an example, winter wheat and bare soils have really close spectral properties because winter wheat has just a small vegetation cover throughout winter. Moreover, identifying land cover on small parcels that do not exceed the spatial coverage of a 250m pixel decrease probability of discriminating land cover by MODIS images.

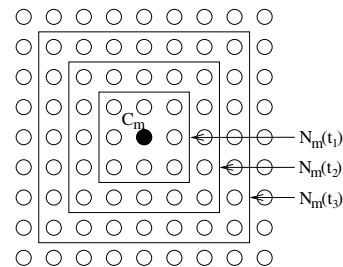


Fig. 1. The Kohonen's Self Organizing Map and topological neighborhood $N_{m_x}(t_i)$ ($t_1 < t_2 < t_3$) of the winning neuron C_{m_x} .

Many methods have been used in the literature to solve similar problems. Authors in [5] used Change Vector Analysis (CVA) in multitemporal space to detect and categorize land-cover change processes, in a region of west Africa, using multitemporal images obtained by Advance Very-High Resolution Radiometer (AVHRR) data. They applied the CVA to the NDVI, as a biomass indicator, calculated from the AVHRR time series data. The series data contained over 100 relatively cloud and smoke-free images that cover the period of 2 years. Authors in [6] used a CVA in the red and near-infrared reflectance space.

We here propose the SOM to carry out the classification and characterization of land covers in the winter season in the Brittany region in France. This region is almost covered by clouds in the winter. So, few and irregular MODIS images may be used to carry such a study.

The following section describes the SOM. Section III presents the data, application and results. Section IV concludes.

II. PRINCIPLE OF THE SOM

There exist many versions of the SOM, the basic philosophy, however, is very simple and already effective. SOM defines a mapping from the input data space n onto a regular one or two-dimensional array of M nodes (see fig. 1). With every node m , a reference vector $C_m \in ^n$ is associated. An input vector $x \in ^n$ is compared with the C_m , and the best match is defined as "response": the input is thus mapped onto this location.

One might say that the SOM is a "nonlinear projection" of the probability density function of the high-dimensional input data onto the two-dimensional array [7]. Let $\mathbf{x} \in \mathbb{R}^n$ be an input data vector. It may be compared with all the \mathbf{C}_m in any metrics; in practical applications, the smallest of the Euclidean distance $\|\mathbf{x} - \mathbf{C}_m\|$ is usually used to define the best-matching node, denoted by the subscript $m_{\mathbf{x}}$:

$$\|\mathbf{x} - \mathbf{C}_{m_{\mathbf{x}}}\| = \min_{m \in \{1, \dots, M\}} \|\mathbf{x} - \mathbf{C}_m\|. \quad (1)$$

Thus \mathbf{x} is mapped onto the node $m_{\mathbf{x}}$ relatively to the values \mathbf{C}_m . An "optimal" mapping would be the one that maps the probability density function $p(\mathbf{x})$ in the most "faithful" fashion, preserving at least the local structures of $p(\mathbf{x})$. During the learning stage, these nodes which are close to each other on the SOM will learn from the same input. The values of the \mathbf{C}_m can be found as convergence limit of the learning process (2), where the initial values of the $\mathbf{C}_m(0)$ can be fixed arbitrary, e.g., randomly:

$$\mathbf{C}_m(t+1) = \mathbf{C}_m(t) + h_{m, m_{\mathbf{x}}}(t)[\mathbf{x}(t) - \mathbf{C}_m(t)]. \quad (2)$$

In (2), t is the time parameter (*i.e.* the number of iterations), and $h_{m, m_{\mathbf{x}}}(t)$ the so-called *neighborhood kernel*. It is a function defined over the lattice points; usually $h_{m, m_{\mathbf{x}}}(t) = h(d(m, m_{\mathbf{x}}), t)$ where $d(m, m_{\mathbf{x}})$ is the distance between the location of \mathbf{C}_m and $\mathbf{C}_{m_{\mathbf{x}}}$ on the SOM. While increasing $d(m, m_{\mathbf{x}})$, or increasing t , $h_{m, m_{\mathbf{x}}}(t)$ decreases monotonically to 0. The average width and the form of $h_{m, m_{\mathbf{x}}}$, defines the "stiffness" of the "elastic surface" to be fitted to the data set.

Let their index in the neighborhood of $m_{\mathbf{x}}$ be denoted by the set $N_{m_{\mathbf{x}}}(t)$.

$$h_{m, m_{\mathbf{x}}}(t) = \begin{cases} \alpha(t) \exp\left(-\frac{d(m, m_{\mathbf{x}})}{2\sigma^2(t)}\right) & \text{if } m \in N_{m_{\mathbf{x}}}(t), \\ 0 & \text{if } m \notin N_{m_{\mathbf{x}}}(t). \end{cases}$$

The value of $\alpha(t)$ is then identified with a *learning-rate factor* ($0 < \alpha(t) < 1$). Both $\alpha(t)$ and the radius of $N_{m_{\mathbf{x}}}(t)$ are usually decreasing monotonically in time (during the ordering process). To obtain almost sure convergence, $\alpha(t)$ must verify [8]:

$$\sum_{t=0}^{+\infty} \alpha(t) = +\infty, \text{ and } \sum_{t=0}^{+\infty} \alpha(t)^2 = A < +\infty,$$

$\sigma(t)$ defines the width of the neighborhood; it corresponds to the radius of $N_{m_{\mathbf{x}}}(t)$ above. In our application we used $\alpha(t)$ and $\sigma(t)$ which begin with their initial values and vanish with time. Typically, $\alpha(t) = \alpha(t-1)\left(\frac{\text{length}-t}{t}\right)$ and $\sigma(t) = \sigma(t-1)\left(\frac{\text{length}-t}{t}\right)$, where 'length' is the training length.

III. APPLICATION AND RESULTS

In this study, three different experiments have been done to characterize and classify the study zone. In the following subsections, we introduce MODIS data used for this application and the high resolution SPOT and Landsat data used for validation. Then, different experiments and their results are presented.

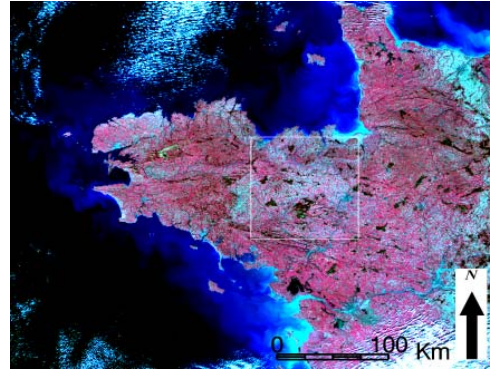


Fig. 2. MODIS image of Brittany (France) on 2/14/2001, RGB: NIR, Red, Green. The rectangle shows the study zone.

A. Data

1) *MODIS data*: MODIS images of winter 2000-2001 were selected according to sensor zenithal viewing angle and cloud coverage criteria. Concerning zenithal viewing angle selection, images acquired with an orbit track centered on Brittany and a radius of 200 km were selected. Low zenithal viewing angle values, inferior to 20, were selected only to avoid spatial resolution variations. Only 4 cloudfree images were available during winter season of 2000-2001. Images were acquired on 11/14/2000, 01/13/2001, 02/14/2001 (see fig. 2) and 05/21/2001. The first seven bands (VIS-IR) of MODIS sensor are atmospherically corrected using 5S model [9]. Only red and near infrared bands at 250m spatial resolution are used to classify land cover in Brittany considering that landscape is fragmented in small parcels and the use of 500m bands will increase mixing effects. Moreover, their spectral information are suited for studying vegetation covers [10].

2) *High resolution data*: Two high resolution mosaics are used for validation. The first high resolution mosaic (see fig. 3) is composed of four SPOT images acquired during January and February 2001: one image acquired on 01/08/2001, two images acquired on 01/14/2001 and one image acquired on 02/14/2001. The second mosaic is constituted of two Landsat ETM+ images acquired on 05/12/2001 and a Landsat image acquired on 05/21/2001. High resolution images are atmospherically corrected using 5S model prior to any process and next corrected from geometric distortion. Mosaicking is done by calculating a linear relation on overlapping regions to avoid spatial variations of reflectance values between images. Each mosaic is classified by maximum likelihood using green, red, near infrared and middle infrared bands to identify forest, water, urban areas, heath, bare soils and vegetation covered fields. Winter cover crops are then identified by combining classifications of SPOT and Landsat mosaics. Fields identified as bare soils in January and May are considered to be bare soil during the whole winter whereas fields identified as bare soils in January and covered in May are considered to be cereals other than corn. Fields identified as covered in January and May are classified as meadows. Finally, fields classified as covered soils in January and bare soils in May are considered

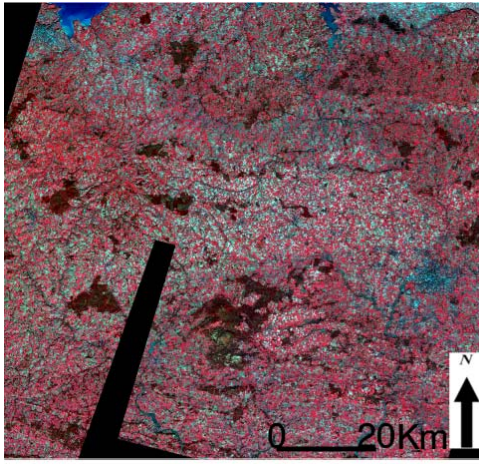


Fig. 3. SPOT images mosaic of Brittany (France), January 2001, RGB: NIR,Red,Green

TABLE I
HYPOTHETICAL CLASSIFICATION OF SOIL OCCUPATION

Class	SPOT image	
	January 2001	Mai 2001
Bare soil	non-vegetated	non-vegetated
Meadows	vegetated	vegetated
Cereals	non-vegetated	vegetated
Winter crops	vegetated	non-vegetated

to be intercrop. Table I shows this process of classifying the winter cover crops. It results an overall accuracy of 90.97% compared to field data.

B. SOM experiments

A SOM of 10×10 nodes has been trained and labeled using a set of multitemporal spectral signatures (training set). These samples have been collected from the study zone by the help of the high resolution data classification images. These later classifications are aggregated by selecting the class majority for each 250m pixel in order to limit point spread function effects [11]. The training set is composed of MODIS pixels that have a purity up to 90% (90% of its corresponding high resolution pixels has the same class).

Due to the small number of pure pixels for validation, another set of MODIS pixels that have a purity up to 75% are used for the validation (validation set). Validation process has been verified on pixels that have the same cover, in the high resolution data, on January 2001 and May 2001. These types are: bare soils, urban areas, forests and meadows. Other land cover types, which classified hypothetically from high resolution data (cf. table I) may lead to validation errors. This is because MODIS data series presents information between January and May 2001 which are not available in the high resolution data. Pixels that have not been changed from January to May, were considered to not changed in between. The SOM work was carried out by using the SOM toolbox

TABLE II
CLASSIFICATION ACCURACY WHEN TRAINING SOM ON ALL THE INPUT DATA

Class	Prod. Acc.%	User Acc. %
Bare soil	70.41	46.19
Meadows	56.12	79.54
Forest	82.37	79.01
Urban	68.98	66.12

TABLE III
CLASSIFICATION ACCURACY WHEN TRAINING SOM ON THE TRAINING SET

Class	Prod. Acc.%	User Acc. %
Bare soil	67.26	51.04
Meadows	64.78	79.10
Forest	80.95	80.66
Urban	79.78	68.17

described in [12]. The different experiments are presented hereafter.

1) *SOM trained on input data*: In this experiment, the SOM was trained on the input data (not the training set) to summarize the input space distribution. Input data were arranged in 8 dimensions, 2 bands for each date. The labeling process was carried out by the training set. Table II shows in columns the ground truth (pixels from high resolution data) and in rows results of MODIS classification image.

The Kappa Coefficient for this classification was 0.5271 while the overall accuracy was 67%. If pure pixels are used for validation, the Kappa coefficient increases to 0.798 and the overall accuracy reaches 88.6%

2) *SOM trained on multitemporal spectral signatures*: In this experiments, the SOM was trained and labeled using the training set. Table III shows the results obtained. The Kappa Coefficient was 0.5902 while the overall accuracy was 71.13%. The validation was carried out for pure pixels up to 75%.

3) *SOM trained on spectral signatures*: In this experiment, spectral signatures of land cover types (cf. III-A2) were arranged to fit into 2 dimension input space. In some other words, the input space will contain samples of each cover type for each date. In this way, each pixel may be investigated and analyzed along its time trajectory on the SOM. Fig. 4 shows the trained and labeled SOM along with the time trajectory for 4 pixels that were classified on the 4 dates as the same class. The classification output of a such process is controlled by the number of hits from one pixel to a specific class. In this experiment, if a pixel is classified as different class in each day, the SOM considers that it is not capable to classify this pixel. Table IV shows the results. The overall accuracy was 67.56% with a Kappa coefficient of 0.5270.

C. SOM vs. NDVI

To validate the capacity of SOM to distinguish bare soils from vegetated covers, we compare it versus a simple NDVI

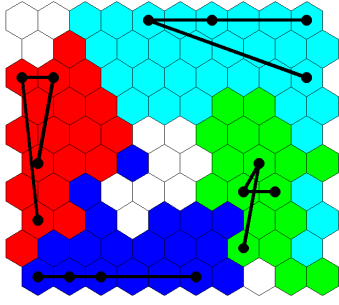


Fig. 4. Time trajectory for MODIS pixels. Four pixels are represented that have the same class throughout winter. Colors are: Blue for bare soils, Red for urban areas, Cyan for forest, Green for meadows

TABLE IV
ACCURACY OF DETECTION WHEN TRAINING SOM SPECTRAL DATA

Class	Prod. Acc.%	User Acc. %
Bare soil	51.91	55.01
Meadows	72.78	71.58
Forest	71.83	81.45
Urban	65.19	57.26

TABLE V
ACCURACY COMPARISON BETWEEN SOM AND NDVI THRESHOLDING

	SOM output %		NDVI output %	
	Prod. Acc.	User Acc.	Prod. Acc.	User Acc.
Bare soil	67.11	71.33	97.62	56.55
Vegetated	88.64	86.49	68.18	100.00
Overall Acc.	82.26		76.95	
Kappa	0.5672		0.5487	

thresholding. The threshold was fixed at 0.55 to distinguish bare soils from vegetated covers [4]. Pixels that have NDVI superior to 0.55 for at least 3 dates in the time series will be considered as vegetated pixels. Pixels with values inferior to 0.55 for at least 3 dates will be considered as bare soil. To avoid low NDVI caused by surface fragmentation, this comparison is conducted on pure pixels (the training set). The SOM used for this comparison is the one used in III-B2, which had the higher overall accuracy. Table V shows results of this comparison. Results show that a SOM has a better overall accuracy and kappa coefficient than that of NDVI for classifying land cover into two classes only; vegetated and bare soils. Results show also a balance between the probability of detection and false alarms for the SOM output.

IV. CONCLUSION AND DISCUSSION

In this study a non-parametric algorithm, the SOM, is used to characterize a fragmented agricultural surface in the Brittany Region in France. The SOM has monitored its capacity to account for temporal evolution of different types of coverages. This method, which depends on training phase on data known *a priori*, may facilitate the analysis process. With algorithms

that depend on determining thresholds, such CVA, a tedious work has to be carried out to analyze the output. From the three presented experiments, a SOM trained on multitemporal spectral data shows higher accuracy than those trained on all input data or on spectral data projected into 2 dimension space.

The validation presented in this work is thought to be degraded by three factors:

- 1) The accuracy of high resolution data classification which was 90%.
- 2) The difference in the acquisition dates between MODIS series and the two high resolution data.
- 3) The fragmentation of the agricultural surface and its effects on pixels used for validation (validation set has pixel purity up to 75%).

Authors think that higher accuracy may be achieved if training and validation data are chosen directly from MODIS data with the help of ground truth maps. Also, the accuracy may be raised by increasing the number of images in the time series.

REFERENCES

- [1] G. Cisci and V. Martinez, "Environmental impact of soil erosion under different cover and management systems," *Soil Technology*, vol. 6, pp. 239–249, 1993.
- [2] J. J. Meisinger, P. R. Shipley, and A. M. Decker, "Using winter cover crops to recycle nitrogen and reducing leaching," in *Conservation Tillage for Agriculture in the 1990's* (J. Mueller and M. Waggoner, eds.), (N. Carolina State Univ.), pp. 3–6, Raleigh, Spec. Bull, 1990.
- [3] S. M. Dabney, J. A. Delgado, and D. W. Reeves, "Using winter cover crops to improve soil and water quality," *Commun. Soil Sci.*, vol. 32, no. 7-8, pp. 1221–1250, 2001.
- [4] R. Lecerf, T. Corpetti, L. Hubert-Moy, and V. Dubreuil, "Monitoring land use and land cover changes in oceanic and fragmented landscapes with reconstructed MODIS time series," in *Third International Workshop on the Analysis of Multi-temporal Remote Sensing Images, Multitemp*, (Biloxi, Mississippi USA), pp. 195–199, May 2005.
- [5] E. F. Lambin and A. H. Strahler, "Change-Vector Analysis in Multi-temporal Space: A Tool to Detect and Categorize Land-Cover change Processes Using High Temporal-Resolution Satellite Data," *Remote Sensing of Environment*, vol. 48, pp. 231–244, 1994.
- [6] X. Zhan, C. Huang, J. Townshend, R. Defries, M. Hansen, C. Dimiceli, R. Sohlberg, J. Hewson-Scardelletti, and A. Tompkins, "Land Cover Change Detection with Change Vector in Red and Near-Infrared Reflectance Space," in *Geoscience and Remote Sensing Symposium Proceedings, 1998. IGARSS'98. IEEE International*.
- [7] T. Kohonen, *Self-Organizing Maps*, vol. 30 of *Springer series in Information Sciences*. Springer, second edition ed., 1997.
- [8] J. Héroult and C. Jutten, *Réseaux neuronaux et traitement du signal*. Collection Traitement du signal, Hermès, 1994.
- [9] D. Tanre, C. Deroo, P. Duhaut, M. Herman, and J. J. Morcrette, "Description of a computer code to simulate the satellite signal in the solar spectrum - The 5S code," *Int. Journal of Remote Sensing*, vol. 11, pp. 659–668, Apr. 1990.
- [10] J. R. G. Townshend, C. O. Justice, W. Li, C. Gurney, and J. McManus, "Global land cover classification by remote sensing: present capacities and future possibilities," *Remote Sensing of Environment*, vol. 35, pp. 243–256, 1991.
- [11] C. Huang, J. Townshend, S. Liang, S. Kalluri, and R. Defries, "Impact of sensor's point spread function on land cover characterization, assessment and deconvolution," *Remote Sensing of Environment*, vol. 80, pp. 203–212, 2002.
- [12] J. Vesanto, J. Himberg, E. Alhoniemi, and J. Parhankangas, "Self-organizing map in Matlab: the SOM Toolbox," in *Proceedings of the Matlab DSP Conference 1999, Espoo, Finland, November 16-17*, pp. 35–40.